Area operators for edge detection

Scott T. Acton *, Dipti Prasad Mukherjee [1]

Oklahoma Imaging Laboratory, School of Electrical and Computer Engineering, Oklahoma State University, 202 Engineering South, Stillwater, OK 74078-5032, USA

Received 28 July 1999; received in revised form 15 February 2000

Abstract

In area morphology, the area open–close (AOC) and close–open (ACO) operations are based on filtering the connected components in the image level sets. Unlike traditional morphology that enforces the shape of the structuring element on image region boundaries, area morphology allows removal of small features without boundary distortion. This study defines ascending and descending objects that depend on the area of the connected components of the level sets. The major contribution of the paper is to define image edges at the boundaries of the ascending and descending objects. From this area morphology approach, thin, closed contours are provided that are suitable for use in image segmentation. A notable strength of the area morphology edge detector is that it does not require the use of a threshold. The edge maps are Euclidean invariant and causal, and yield good performance in terms of edge localization and the suppression of below-scale detail. The results demonstrate the superior performance of the area operator-based edge detection over the conventional techniques.

Keywords: Non-linear filters; Edge detection; Segmentation

1. Introduction

Estimation of an edge map of a scene is a well-researched topic in pattern recognition and related fields. Various edge detection schemes have been developed that provide moderate to good result in segmenting images (Jain et al., 1995). In this initiative, we explore the application of area morphology to the problem of edge detection. To date, the area morphology operators have been utilized primarily in image filtering, enhancement and reconstruction (Salembier and Serra, 1995).

Area operators are based on the properties of connected components within the image level sets. In the present application, we have utilized the area property of the connected components (essentially the number of pixels in a particular connected component). The major advantage of area morphology, which is revealed in the edge detection results, is that, unlike standard morphology, area morphology does not impose the shape of a structuring element on the constituent image regions.

At the onset, we define the terms used in the proposed edge detection technique. It is well known that a perceptually relevant edge map is a

function of image scale (Marr, 1982). For the present approach, we would also like to detect edges at predefined image scales such that unnecessary image details irrelevant for semantic interpretation could be excluded from the final result. However, in other scale-sensitive edge filters, this is achieved at the cost of edge localization error and distortion in the edge map (Marr and Hildreth, 1980; Torre and Poggio, 1986). Other edge detectors produce undesirable artifacts such as fragmented edge segments or thick edges that require expensive and heuristic post-processing.

In contrast, area-based edge operators do not produce edge localization error or edge distortion. The connected invariant area operators remove or preserve connected components in their entirety. In this way, regions are not distorted in part. The preservation of a given feature depends on feature area only. The area operators not only provide a scaling for edge detection but also eliminate spurious regions due to noise.

Here, connected invariant operators are introduced that provide a multi-scale image representation. Within the image representation, ascending and descending objects are defined. Edges are extracted by locating the boundary between ascending and descending object pixels in the processed imagery. We have shown that desirable properties such as Euclidean invariance and causality, relevant for any edge detection scheme, are maintained for the proposed method. Other important aspects of the proposed algorithm include edge contiguity, edge thinness, and independence from thresholds.

The paper is organized as follows. First, definitions and operators necessary for description of the edge detection method are provided in Section 2. This discussion is followed by the description of the edge detection technique in Section 3. Results for a number of images and comparison with results of other multi-scale edge detection schemes are provided in Section 3, with conclusions in Section 5.

2. Definitions

We start with the definition of image level sets and the associated connected components. These definitions are followed by the specification of the area morphology operators.

Definition 1. For a discrete domain image $I \subset Z^2$ and image location p, level set s at l, $l \in [0, L]$, is defined by

$$s(p) = \begin{cases} 1 & \forall p : I(p) \geqslant l, \\ 0 & \text{otherwise.} \end{cases} \tag{1}$$

Therefore, the level set is a binary image representation of the image at a specified intensity level.

Definition 2. For a level set s (at level l) and an image location p, the connected component $C_s(p)$ at p is given by

$$\boldsymbol{C}_s(p) = \{q : \exists P_{I \geqslant l}(p, q)\}, \tag{2}$$

where $P_{I \geqslant l}(p, q)$ is an unbroken path between image locations p and q for which $s(\cdot) = 1$ (hence $I(\cdot) \geqslant l$). The neighboring elements in such a path are defined by 4 or 8 connectivity.

Definition 3. For level set s, an *area–open* operation is defined as

$$s \circ (a) = \{p : \exists |\boldsymbol{C}_s(p)| \geqslant a\}. \tag{3}$$

The area of the connected component is given by the cardinality $|\boldsymbol{C}_s(p)|$, and a is the minimum area specified for area open. Therefore, an area-opened level set does not contain connected components of size less than the prescribed area.

Definition 4. Similarly, for level set s, an *area-close* operation is defined as

$$s \bullet (a) = \{p : \exists |\boldsymbol{C}_s^{\sim}(p)| \geqslant a\}. \tag{4}$$

In case of area-close with specified area a, the cardinality $|\boldsymbol{C}_s^{\sim}(p)|$ of the connected component is defined in the complement of level set s, that is, where $s(p) = 1\ \forall p : I(p) < l$. Again, area-closed level sets do not contain connected components (of zeros) that do not meet the minimum area.

Sequential application of area-open and area-close operation results in useful multi-scale operators. Area open–close (AOC) and area close–open (ACO) are represented as $s \bullet (\circ(a))$

and $s \circ(\bullet(a))$, respectively. Both operations remove connected components with area less than a from a level set and the complemented level set.

An area-scaled image is reconstructed via stacking of processed level sets. The reconstructed area-scaled image $\boldsymbol{I}_r^a$ at scale a, is given by

$$\boldsymbol{I}_r^a = \sum_{l=0}^{L} s^l(l), \tag{5}$$

where $s^l(l)$ is the AOC-processed (or ACO-processed) version of level set $s(l)$ for area a.

Before we detail the area morphology edge detection technique, we present some of the important properties of area morphology relevant to edge detection process. For a unique input image $\boldsymbol{I}$ and scale a, the AOC and ACO operations generate a unique sequence of scaled images $\boldsymbol{I}_r^a$ for $a \geqslant 0$, since $a = 1$ gives the input image. Also, AOC and ACO operations are invariant to Euclidean transformation. Since AOC and ACO retain or remove connected components of a specified area (i.e., they are connected invariant), the translation and rotation of the original image does not distort the area-scaled reconstructed image (excluding discretization error). These properties are relevant in context of edge detection as the detected edge map should be invariant to translation and rotation.

An additional property relevant to edge detection is causality. Satisfying the causality property guarantees that the filtered image at any particular area scale depends only on the "previous" scale. This is true for a sequence of AOC or ACO operations if we create the sequence by performing AOC (or ACO) in a successive manner. With the AOC operation, the construction of image $\boldsymbol{I}_r^{a_1}$ is dependent only on $\boldsymbol{I}_r^{a_2}$ using $\boldsymbol{I}_r^{a_1} = \boldsymbol{I}_r^{a_2} \bullet (\circ(a_2))$ for $a_1 \geqslant a_2$. A similar causal construction is used for the ACO operation. Given the AOC and ACO framework, we present the area morphology edge detection method.

3. Edge detection

Ideally, we seek the potential edge points that represent boundaries between image objects. However, the term *object* itself is not defined. To tackle this problem, we introduce two types of objects that are defined by connected components within the image level sets.

Definition 5. The connected components that represent *ascending* objects, $\boldsymbol{C}^{\cup}(p)$, and *descending* objects, $\boldsymbol{C}^{\cap}(p)$, are defined as follows. For an area-scaled image $\boldsymbol{I}_r^a$, the potential ascending object at image location p is given by $\boldsymbol{C}^{\cup}(p) = \{q : \exists P_{I \geqslant l}(p,q)\}$ where $P_{I \geqslant l}$ is the path defined in (2). The potential descending object is $\boldsymbol{C}^{\cap}(p) = \{q : \exists P_{I \leqslant l}(p,q)\}$. We say that the object at point p is ascending if $|\boldsymbol{C}^{\cup}(p)| < |\boldsymbol{C}^{\cap}(p)|$ and is descending if $|\boldsymbol{C}^{\cup}(p)| > |\boldsymbol{C}^{\cap}(p)|$.

For a given image location, transitions from the ascending to descending objects and vice versa are defined as potential edge points. These transitions are detected by locating zero crossings of the cardinality of the ascending and descending connected components

$$Z(p) = |\boldsymbol{C}^{\cup}(p)| - |\boldsymbol{C}^{\cap}(p)|. \tag{6}$$

The zero crossings are detected with respect to the four neighbors of every pixel in the images processed by AOC or ACO.

In the next section, we present a set of results obtained after detecting the zero crossings in (6). The results are compared with other scale-sensitive edge detectors, viz., the Laplacian-of-a-Gaussian (LoG) (Marr and Hildreth, 1980) and Canny's edge detector (Canny, 1986).

4. Results

Edge detection results using area operators and comparisons to traditional edge operators are presented in this section. Note that the primary objective of the proposed edge detector is to detect edges relevant for pattern recognition. Appropriate scales are selected to detect meaningful object boundaries for which post-processing is not required, providing semantic interpretation of object shapes. Therefore, unnecessary image details and

noise should be removed in the scaling/filtering process.

We start with the wrench image example in Fig. 1. Fig. 1(b) shows a noisy (5% salt and pepper noise) version of Fig. 1(a). Fig 1(c) contains the AOC result for Fig. 1(b) at scale $a = 200$, while Fig. 1(d) is the corresponding edge map using the zero crossings computed with (6). Notice the localized and dominant edge information in the noiseless background of Fig. 1(d). Compare this result with that of Figs. 1(e) and (f), where LoG edges of Fig. 1(b) are presented at two different scales. In the case of Fig. 1(e), the standard deviation of the Gaussian is $\sigma = 2$ with an edge intensity threshold set at $t = 0.5$ (for intensity scale normalized between 0 and 1). For Fig. 1(f), a low threshold of $t = 0.1$ is chosen at a coarser scale $\sigma = 3$. A lower value for σ results in retention of irrelevant details, while higher values for σ lead to significant edge distortion, already evident in the case of Fig. 1(f). For further comparison, the edge map of Fig. 1(g) is given using Canny's edge algorithm (Canny, 1986). Broken edge pixels (*edgels*) and noise sensitivity are two drawbacks of the Canny result. A more efficient implementation of the Canny approach is given by Deriche (1987).

The microscopic image of blood plasma in Fig. 2 appears to be a simple image for edge detection at a glance. However, since our objective is to detect a single significant boundary present in the

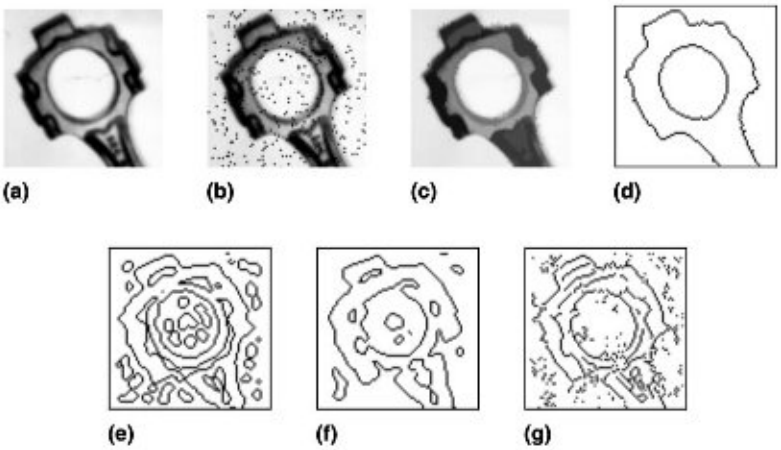

Fig. 1. (a) Original wrench image (80×80), (b) corrupted image with 5% salt and pepper noise, (c) AOC-scaled image of (b) at $a = 200$, (d) edge map of (c) using (6), (e) LoG edge map at $\sigma = 2$ and $t = 0.5$, (f) LoG edge at $\sigma = 3$ and $t = 0.1$, (g) edge map following the Canny algorithm (Canny, 1986) at $\sigma = 1$.

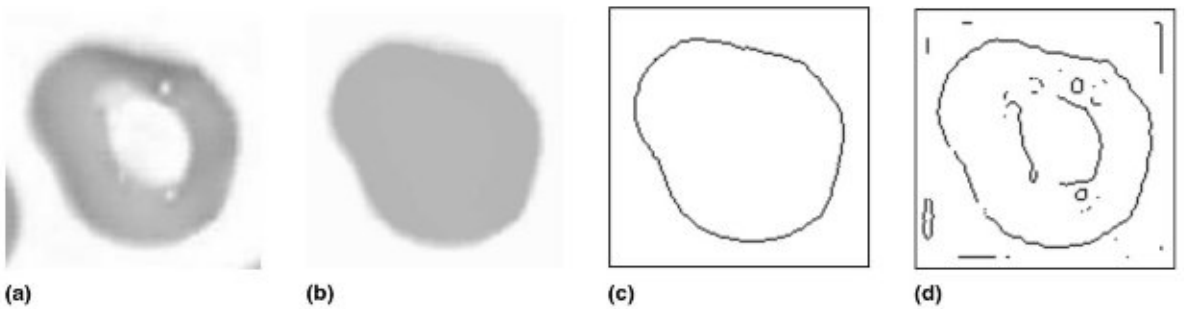

Fig. 2. (a) Blood plasma image (129×129), (b) AOC-scaled image at $a = 4000$, (c) edge map of (b) using (6), (d) LoG edge map at $\sigma = 2$ and $t = 0.5$.

image (in order to count the cells and measure their area, for example) avoiding the intensity variation in the center of the cell (which is due to illumination), the traditional edge detectors do not suffice. The proposed area morphology edge algorithm can detect the accurate localized and connected edge map of the blood cell as shown in Fig. 2(c) after area scaling the original image at $a = 4000$ as shown in Fig. 2(b). The LoG edge shown in Fig. 2(d) is disconnected at $\sigma = 2$ and $t = 0.5$. Again, in case of the LoG operator, there exists a compromise between unnecessary details and contiguity of the edge map.

In the case of Fig. 3(a), we would like to obtain an edge map that conveys the major semantic contours of the object, namely that of the tire and rim. Fig. 3(b) shows the area morphology edge map at $a = 800$. In contrast, the LoG edge map of Fig. 3(c) reveals edge distortion and an overabundance of detail that would require extensive post-processing for meaningful interpretation.

Further examples are provided using the cameraman and printed circuit board images as shown in Figs. 4 and 5, respectively. Fig. 4(b) gives the result of AOC of the cameraman image from Fig. 4(a) at $a = 100$. Fig. 4(c) provides the result of area morphology based edge map, while Fig. 4(d) is the edge map due to the Canny edge detection algorithm. Similarly, the edge image of printed circuit board of Fig. 5(a) is shown in Fig. 5(c) after AOC operation at area 25 as shown in Fig. 5(b). Again the output of the Canny algorithm is shown in Fig. 5(d). In case of both Figs. 4(d) and 5(d), the standard deviation for Gaussian is taken as 0.5. In both the examples, significant linear structures are extracted using area morphology-based edge detection technique without major distortion to other features such as corners.

Selection of the appropriate edge detection algorithm in most cases is domain specific. Moreover, selection of parameters involved in any specific edge algorithm is a non-trivial task. For example, results obtained in cases of Figs. 1(e)–(g) or 2(d) or 3(c), etc. could be improved with further experimentation of threshold and standard deviation values. However, in such traditional methods,

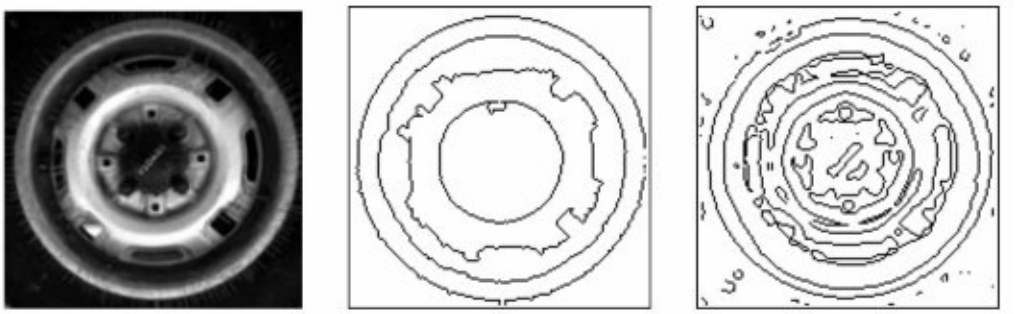

Fig. 3. (a) Tire rim image (150×150), (b) edge map of (a) using AOC at $a = 800$, (c) LoG edge map at $\sigma = 2$ and $t = 0.5$.

Fig. 4. (a) Cameraman image, (b) after AOC operation on (a) at $a = 100$, (c) edge image from (b) using (6) (edges shown in white), (d) edge map using (Canny, 1986) at $\sigma = 1$.

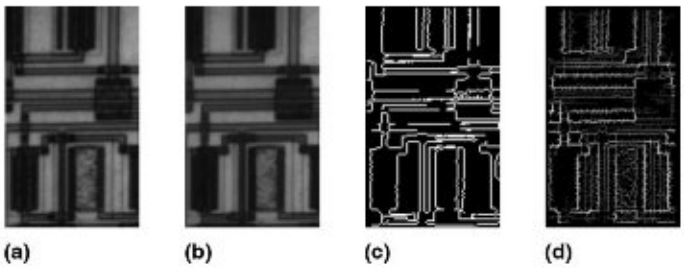

Fig. 5. (a) Circuit board image, (b) after AOC operation on (a) at $a = 25$, (c) edge image from (b) using (6) (edges shown in white), (d) edge map using (Canny, 1986) at $\sigma = 1$.

it would be difficult to eliminate unnecessary details, especially the detail present in Figs. 2(d) and 3(c) without further post-processing. Moreover, the proposed method is superior in context of edge shift and feature distortion that are unavoidable in convolution based methods.

The edge maps computed using area morphology, the Canny method and the LoG are further compared by calculating the percentage of missing and excess edgels. These are calculated based on ground truth contour maps. The percentage of missing edgels, $\boldsymbol{m}$, represents the ratio of the number of edgels missing with respect to the number of edgels in the ideal contours. Similarly, the percentage excess edgels, $\boldsymbol{e}$, represents the ratio of number of excess edgels with respect to the ideal number of edgels. The excess edgels represent unnecessary details and edgels to due to noise. The results, tabulated in Table 1, show that the area-based edge operator clearly outperforms the other edge detectors in terms of these metrics.

One of the limitations of the present method is that weak edges could not be differentiated against perceptually significant edges. We are presently investigating the extension of the area morphology edge detector to cases where "weak" edges are removed at each scale. This edge evaluation could be achieved by combining both edges from area morphology along with the intensity edge strength, realized through a gradient magnitude calculation. For the image of blood cells shown in Fig. 6(a), Fig. 6(b) is the area-scaled

Table 1
Objective comparison of AOC-based edge maps, LoG, and Canny edge maps[a]

	1(d) AOC	1(e) LoG	1(f) LoG	1(g) Canny	2(c) AOC	2(d) LoG	3(b) AOC	3(c) LoG	4(c) AOC	4(d) Canny	5(c) AOC	5(d) Canny
$\boldsymbol{m}$ (%)	<1	2.1	3.6	7.7	<1	2.3	17	24	9	14	6	8
$\boldsymbol{e}$ (%)	<1	268	108	189	<1	96	<1	96	12	7	4	34

[a] Here, $\boldsymbol{m}$ and $\boldsymbol{e}$ represent percentage of missing and excess edgels, respectively. The percentages are calculated with respect to the number of edgels in the ground truth contours.

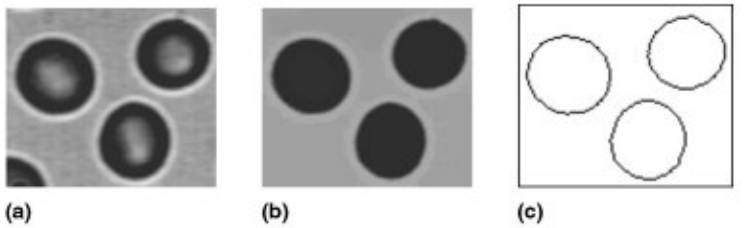

Fig. 6. (a) Blood cells image (91 × 106), (b) after AOC on (a) at $a = 500$, (c) edge map derived from the combination of gradient magnitude and edges from the AOC.

image at scale 500. An edge map derived from a logical AND of the edges from area morphology and the edges from the gradient magnitude is shown in Fig. 6(c). Note that this introduction of edge strength at a particular scale brings the edge localization and perceptual integrity together in the same framework.

Using the connected component labeling approach, the process of AOC (or ACO) imposes a computational cost of $O(LN)$ comparisons where L is the number of intensity levels ($L = 256$ in the examples presented in Section 4) and N is the number of pixels that need to be processed in a connected component analysis. However, a number of measures can be implemented to reduce both the space and time complexity of area morphology process (Vincent, 1993). To detect edges based on the length of connected components of the ascending or descending objects, only an additional $O(N)$ operations are necessary.

In the next section, we conclude by indicating the potential application domain of the current approach.

5. Conclusions

We have shown that the proposed edge detection technique can detect edges sufficient for semantic interpretations without post-processing such as edge-linking or edge-filtering. The approach is based on a scale-sensitive filtering process that leads to edge maps of the prescribed scale. Note that the entire process is devoid of any threshold selection, in contrast to traditional edge detection techniques. The area morphology edge detection method is currently being used in two multi-media applications: content-based retrieval and object-based coding.

References

Canny, J., 1986. A computational approach to edge detection. IEEE Trans. PAMI 8 (6), 679–698.

Deriche, R., 1987. Using Canny's criteria to derive a recursively implemented optimal edge detector. Internat. J. Comput. Vision 1 (2), 167–187.

Jain, R., Kasturi, R., Schunck, B., 1995. Machine Vision. McGraw-Hill, New York.

Marr, D., 1982. Vision. Freeman, San Francisco.

Marr, D., Hildreth, E., 1980. Theory of edge detection. Proc. Roy. Soc. London B 207, 187–217.

Salembier, P., Serra, J., 1995. Flat zones filtering, connected operators and filters by reconstruction. IEEE Trans. Image Process. 4 (8), 1153–1160.

Torre, V., Poggio, T.A., 1986. On edge detection. IEEE Trans. PAMI 8, 147–163.

Vincent, L., 1993. Morphological gray scale reconstruction in image analysis: applications and efficient algorithms. IEEE Trans. Image Process. 2 (2), 176–201.